Published in final edited form as:
Magn Reson Med. 2014 December ; 72(6): 1522–1529. doi:10.1002/mrm.25477.

Ungated Radial Quiescent-Inflow Single-Shot (UnQISS) Magnetic Resonance Angiography Using Optimized Azimuthal Equidistant Projections

RR Edelman[1,2], **S Giri**[3], **IG Murphy**[2], **O Flanagan**[2], **P Speier**[4], and **I Koktzoglou**[1,5]

[1]NorthShore University HealthSystem, Evanston, USA

[2]Feinberg School of Medicine, Northwestern University, Chicago, USA

[3]Siemens Healthcare, Chicago, USA

[4]Siemens AG Healthcare Sector, Erlangen, Germany

[5]The University of Chicago Pritzker School of Medicine, Chicago, USA

Abstract

Purpose—We hypothesized that a non-contrast-enhanced MR angiogram (NEMRA) could be acquired without cardiac gating by using a variant of the Quiescent-Inflow Single-Shot (QISS) technique.

Methods—Ungated QISS (UnQISS) MRA was evaluated in eight patients with peripheral arterial disease at 1.5 Tesla. The radial acquisition used optimized azimuthal equidistant projections, a long quiescent inflow time (1200 ms) to ensure replenishment of saturated in-plane spins irrespective of the cardiac phase, and a lengthy readout (1200 ms) so that a complete cardiac cycle was sampled for each slice. Venous and background tissue suppression was obtained using frequency-offset-corrected inversion radiofrequency pulses.

Results—Scan time for UnQISS was 15.4 minutes for an 8-station whole-leg acquisition. The appearance of UnQISS MRA acquired using the body coil was comparable to ECG-gated QISS MRA using phased array coils. A small radial view angle increment minimized eddy current-related artifacts, whereas image quality was inferior with a golden view angle radial increment or Cartesian trajectory. In patient studies, ≥50% stenoses were consistently detected.

Conclusion—Using UnQISS, peripheral NEMRA can be obtained without the need for cardiac gating. The use of fixed imaging parameters and body coil for signal reception further simplifies the scan procedure.

Introduction

The availability of accurate noninvasive imaging tests has decreased the need for preoperative digital subtraction angiography in the evaluation of peripheral arterial disease (PAD). Although highly accurate, contrast-enhanced magnetic resonance angiography

Corresponding Author: Robert R. Edelman, M.D., Department of Radiology, NorthShore University HealthSystem, 2650 Ridge Avenue, Evanston, IL 60201, Tel: 847-570-2553, Redelman999@gmail.com.

(CEMRA) is contraindicated in patients with severely impaired renal function.[1] Non-contrast-enhanced MRA (NEMRA) techniques include both flow-independent[2] and flow-dependent[3,4] varieties, with the latter in more widespread use.[5] Current flow-dependent techniques for peripheral NEMRA such as subtractive fast spin echo[6], flow-sensitive dephasing[7], and QISS MRA[8] typically require the use of cardiac gating to synchronize data acquisition to specific phases of the cardiac cycle. As a consequence, they are primarily useful in patients with adequate electrocardiographic (ECG) tracings and regular heart rhythms. Moreover, given the need for imaging with a high signal-to-noise ratio (SNR) over a large region, a peripheral vascular phased array coil is generally used.

We propose an ungated variant of quiescent-inflow single-shot MRA (*UnQISS*) that eliminates the need for cardiac gating. Moreover, the use of a peripheral vascular phased array coil is optional. UnQISS MRA is similar to QISS MRA in applying an RF pulse to suppress in-plane background signal and then relying on the quiescent interval (QI) to provide for refreshment with fresh arterial spins. Both techniques acquire stacks of thin 2D slices, use an alpha/2 spin preparation, bSSFP single-shot readout, and apply an RF pulse to suppress venous signal. In this pilot study, UnQISS was compared with QISS and/or CEMRA in healthy subjects and patients with PAD.

Methods

The study was approved by the Institutional Review Board and used written, informed consent. Imaging was performed on a 1.5 Tesla system (Magnetom Avanto, Siemens AG, Erlangen, Germany) with peak gradients and slew rates of 45 mT/m and 200 T/m/s. A prototype of the UnQISS MRA pulse sequence was developed and optimized in six healthy subjects (5 male, age range 34–67). Comparison of QISS MRA and the optimized UnQISS technique was performed in eight patients with PAD (5 male, age range 58–82). In 5 of 8 PAD patients with sufficient renal function (GFR ≥ 30 mL/min/1.73 m^2) to receive gadolinium-based contrast material, comparisons were also made with stepping-table CEMRA using an imaging protocol previously described.[8]

QISS MRA

For ECG-gated QISS MRA, a Cartesian k-space trajectory was used with one slice per RR interval and other imaging parameters as described previously.[9] The QI allows for inflow of fresh arterial spins after the application of an in-plane radiofrequency (RF) saturation pulse. The QI of 228 ms corresponds to a TI (time from the in-plane saturation RF pulse to the center of k-space) of 350 ms.

UnQISS MRA

Current NEMRA techniques generally require data collection to be synchronized with the cardiac cycle using ECG or pulse gating. For instance, with standard time-of-flight peripheral MRA, cardiac gating is needed to avoid ghost artifacts from periodic view-to-view variations in arterial signal.[10] Without gating, ghost artifacts degrade image quality. In the case of subtractive techniques like fresh-blood imaging or flow-sensitive dephasing, cardiac gating is essential to ensure that data are specifically acquired during peak systolic

and diastolic phases of the cardiac cycle. For QISS MRA, cardiac gating ensures that data are collected during slow diastolic flow, since the balanced steady-state free-precession (bSSFP) readout is prone to artifacts when data are collected during rapid, accelerating flow in early systole.[11]

We hypothesized that QISS MRA could be acquired without the need for cardiac gating. However, an ungated implementation must overcome several challenges. For instance, QISS MRA applies an RF saturation pulse to the imaging slice in order to suppress signal from background spins, and another inferiorly in order to suppress signal from venous spins. With ECG-gated QISS MRA, the QI is always synchronized to the period of rapid systolic forward flow, thereby ensuring complete replenishment of saturated in-plane arterial spins by unsaturated ones. Without cardiac gating, the RF saturation pulses may be applied during any phase of the cardiac cycle, and the cardiac phase is unpredictably different for each slice. Consequently, full replenishment of saturated in-plane arterial spins is no longer guaranteed. Moreover, the bSSFP data acquisition may occur during any cardiac phase as well, including during early systole when flow artifacts are likely. Given the presence of triphasic flow in healthy peripheral arteries, imaging during periods of retrograde flow also has the potential to cause artifacts.

Imaging parameters for QISS and UnQISS are summarized in Table 1 and the technical differences between the two imaging techniques are illustrated in Fig. 1. These differences are as follows:

1. Without cardiac gating, the application of the in-plane RF saturation pulse will overlap a random phase of the cardiac cycle. Moreover, this cardiac phase will unpredictably vary from slice to slice. If the saturation pulse overlaps early diastole, then (depending on the length of the cardiac cycle) there may be inadequate refreshment of saturated in-plane arterial spins for many hundreds of milliseconds. In order to ensure full replenishment of in-plane spins for every slice, irrespective of the cardiac phase when the saturation pulse is applied and allowing for physiological variations in heart rate, the QI is lengthened to exceed the duration of the cardiac cycle.

2. As a consequence of the longer QI (and TI), in-plane background tissue and venous signals must be suppressed with inversion pulses rather than saturation pulses. Moreover, given the longer period for venous inflow, the venous inversion pulse must be applied over a broader region. Based on studies in healthy subjects, a 200-mm-thick inversion region was used (versus a 100-mm-thick saturation region with QISS) in order to avoid having outlying venous spins flow into the slice without being inverted. Conventional hyperbolic secant adiabatic pulses have a relatively poor slab profile and are unsuitable for such large inversion regions. Therefore, a frequency offset corrected inversion (FOCI) pulse[12,13] (pulse duration 10.24 ms, μ=12, β=900, gradient factor of 2.0), which has an improved slice profile, was used.

3. The duration of the bSSFP readout is much longer with UnQISS than QISS MRA. The long readout has two benefits. First, it enhances SNR, partly compensating for the use of the body coil for signal reception instead of a phased array coil. Second,

we assume that a random minority of views for each slice may be acquired during early systole, and therefore show artifactual signal fluctuations. By acquiring data from a complete cardiac cycle for each slice, these artifacts will be diluted by the majority of views acquired during other portions of the cardiac cycle when flow is not rapidly accelerating.

4. An undersampled radial readout is used instead of a Cartesian readout.[14] The radial readout allows the number of views to be changed without affecting spatial resolution and allows greater flexibility in the choice of k-space trajectory. The standard manufacturer-implemented gridding reconstruction algorithm was used. QISS used a parallel acceleration factor (GRAPPA) of 2, whereas no parallel acceleration was used for UnQISS.

5. The view angle increments are selected to ensure uniform azimuthal coverage for the particular number of views while make multiple revolutions around radial k-space. A uniform distribution of views helps to ensure that the minority of views that show artifactual signal fluctuations are distributed over radial k-space rather than occurring in bunches that might cause more artifacts in the reconstructed image (Fig 1). Both golden (≈111.25 degrees) and azimuthal equidistant projections using smaller, numerically optimized view angle increments (ϕ) were evaluated. At the time of our study, ϕ was was computed over a predefined range (e.g. 9–11 degrees for a target angular increment of 10 degrees) using time-consuming numerical simulations. Values for ϕ(in degrees), however, can be quickly computed as $\phi = 180^{*}m/N$ where N is the number of views in the readout, and m is an integer that does not share an integer factor (f) with N, where $f>1$.

6. Given the use of a radial readout and large number of views, conventional fat suppression techniques are ineffective. Consequently, a phase-based reconstruction is used for fat suppression.[15]

Unlike ECG-gated QISS where scan time is predicated on the RR interval, scan time for UnQISS is determined solely by the choice of the shot repetition time (TR), which is approximately equal to the QI plus the readout duration. For a QI of 1200 ms and readout duration of 1200 ms, the shot TR is 2400 ms. Thus scan time for a 384-slice scan (eight stations, 48 slices per station) with this shot TR is 15.4 minutes.

Signal Analysis

The SNR for ECG-gated QISS and UnQISS using the peripheral array coil, and UnQISS using the body coil, were measured in one volunteer at the mid-thigh level. Since Cartesian QISS uses parallel imaging but radial QISS does not, standard SNR measurements are inappropriate. Therefore, noise was estimated by performing four measurements for each technique. A mean data set and a standard deviation data set from these four measurements were constructed on a Leonardo workstation (Siemens AG, Erlangen, Germany). The SNR was computed as the average signal in the artery on the mean data set, divided by the average signal of a soft-tissue region located adjacent to the artery on the standard deviation data set (i.e. noise). Measurements (SNR and contrast-to-noise (CNR)) were obtained at the central slice of each station per QISS sequence. For UnQISS, the measurements were

obtained after phase-based fat suppression was performed. Regions of interest used to measure signal in the artery and adjacent background tissue (muscle, fat) were circular in shape and approximately 0.5 cm and 5 cm in diameter, respectively.

Analysis of Patient Data

For the eight PAD patients, images were reviewed on an off-line workstation (Leonardo; Siemens Healthcare) by a clinical radiologist with 5 years experience interpreting MRA. QISS and UnQISS sequences were examined, and CEMRA for comparison where available (5 out of 8 patients). Images were viewed as original source data (axial thin slice, fat-saturated images) and in coronal maximum-intensity projection (MIP) format. The reader recorded the number, site and percentage of lumen occluded of each stenosis in each patient, and also graded the degree of stenosis according American College of Radiologists (ACR) scoring system, as employed in a previous multicenter clinical trial.[16] Stenosis was graded as follows: a score of 0 = normal patency; 1 = less than 50% stenosis; 2 = one lesion with 50% or greater stenosis; 3 = more than one lesion with 50% or greater stenosis; and 4 = occlusion. In each patient, 31 anatomic arterial segments of the lower extremity arteries were evaluated and scored.[17] The degree of venous signal contamination was also scored from 1 to 4 as follows: 1 = no venous signal; 2 = mild venous signal not interfering with arterial evaluation; 3 = moderate venous signal, not interfering with arterial evaluation; and 4 = prominent venous signal, potentially interfering with interpretation of arterial signal. A kappa (κ) analysis was used to assess inter-sequence agreement in stenosis gradings. Differences in venous signal between UnQISS and QISS sequences were assessed using the Wilcoxon signed-rank test. *P* values less than 0.05 were assumed to indicate statistical significance.

Results

Volunteer Imaging

Based on volunteer studies, a sampling bandwidth of 651 Hz/pixel and 316 radial views were used for UnQISS (compared with a sampling bandwidth of 658 Hz/pixel and 92 Cartesian views for QISS). Arterial SNR for ECG-gated QISS (using phased array coils), UnQISS (using phased array coils), and UnQISS (using the body coil) from one subject in the mid-thigh region were: 38.3, 51.4, and 13.5. The corresponding CNR for artery-fat and artery-muscle were: 35.6 and 31.3 (ECG-gated QISS), 51.4 and 43.4 (UnQISS phased array coil), and 13.5 and 11.4 (UnQISS body coil). (Note that these values are not normalized for scan time, which for UnQISS is typically at least twice as long as for QISS).

Maximum intensity projection images for various pulse sequence implementations tested in volunteers are shown in Fig. 2. Compared with ECG-gated QISS MRA (Fig. 2A), image quality was degraded by horizontal banding artifacts when the same sequence was acquired without ECG gating (Fig. 2B). Similar to ECG-gated QISS MRA, UnQISS MRA using a small azimuthal view increment of $\approx$10 degrees (Fig. 2C) provided excellent display of arterial anatomy, even though the latter used the body coil for signal reception and the former used the peripheral vascular, body and spine phased array coils. UnQISS acquired with a Cartesian k-space trajectory showed severe vessel irregularity (Fig. 2D), with nearly

three times as much arterial signal variation as a radial k-space trajectory (coefficient of variation = 8.5% for radial versus 21.5% for Cartesian). Image quality was overall satisfactory with a golden radial view angle increment but arterial signal loss was observed in diagonally opposite corners of the image (Fig. 2E), due presumably to eddy current effects that worsen with distance from the magnet isocenter. Use of radial UnQISS with a short QI and shot TR resulted in horizontal banding artifacts (Fig. 2F). In general, an UnQISS shot TR/QI on the order of 2400 ms/1200 ms was found to reliably eliminate banding artifacts and give optimal results across all slices.

The azimuthal view angle increment was calculated based on the number of radial views to provide near uniform k-space coverage while keeping the view angle small and making several revolutions around radial k-space within each shot. A non-optimal view angle increment providing non-uniform azimuthal sampling of radial k-space resulted in severe image degradation (Fig. 3).

Whole-leg UnQISS MRA using the body coil for signal reception is shown in Figure 4. Compared with QISS, UnQISS images often showed less uniform suppression of superficial fat signal and therefore required more editing to optimize MIP quality. The peripheral arteries (including small calf arteries) were well shown by both UnQISS and QISS MRA. In some cases, a mild degree of striping artifact was present with UnQISS that was most evident in the calf region, although not to a degree that would mimic stenotic disease. Also, venous signal was absent from QISS MRA, whereas a mild amount of venous signal was generally evident with UnQISS MRA.

Patient Imaging

Patient studies showed good correspondence between QISS and UnQISS (Figure 5). QISS and unQISS sequences were each reviewed in a total of 8 patients (248 segments), and CEMRA was performed and reviewed in 5 out of 8 patients (155 segments). On UnQISS and QISS images, the number of stenoses identified per patient ranged from 1–10 (total n=26). There were no differences between UnQISS and QISS in the grading of stenoses, resulting in perfect agreement ($\kappa = 1.00$, $P < 0.001$). UnQISS and QISS both showed excellent agreement with CEMRA ($\kappa = 0.85$, 95% confidence interval of 0.73–0.97; $P < 0.001$). Differences in ACR stenosis grades between non-contrast MRA (UnQISS and QISS) and CEMRA were seen in five arterial segments. In three of these segments, stenosis was graded as an occlusion on the non-contrast images, but was sub-total (>90%) on CEMRA. Two stenoses identified at CEMRA were not seen by the non-contrast sequences. These two lesions were in the same patient but in different anatomical segments, both of which were ACR grade 2 (single lesion, ≥50% stenosis) at CEMRA. Venous signal contamination was not seen on QISS images, but was seen in all 8 UnQISS images (mean scores of 1.0 ± 0.0 vs 2.7 ± 0.7, respectively; $P < 0.05$). In only one patient was venous signal during UnQISS sufficiently prominent to potentially interfere with interpretation of the arterial tree, but when axial source images were reviewed venous signal did not interfere with arterial signal. No venous signal was observed with CEMRA in the 5 patients who underwent CEMRA.

Discussion

Using UnQISS MRA, we have demonstrated that it is possible to obtain diagnostic quality images of the peripheral arteries without ECG gating. Moreover, the use of a phased array coil is optional unless a high-resolution study (e.g. 1 mm-thick slices) is needed. The basic principles underlying ECG-gated QISS and UnQISS MRA are much the same. However, UnQISS MRA uses a much longer QI and readout duration. Another key modification is the use of an undersampled radial k-space trajectory with optimized azimuthal equidistant projections instead of a Cartesian trajectory. A Cartesian k-space trajectory has the drawback that the central k-space views dominate image contrast. Consequently, any k-space signal fluctuations that occur within these central views will severely degrade the MRA. On the other hand, with a radial trajectory all views are equally weighted in the reconstructed image. Flow-related signal fluctuations that occur in a minority of views are diluted by the intact signals from the remaining views, so that there is only a minor impact on image quality.

Because these signal fluctuations were diluted rather than being eliminated (as is the case with cardiac gating), some residual horizontal striping was sometimes apparent with UnQISS MRA, particularly in the calf region. When present, the striping was mild and often symmetrical in both legs. However, it might be possible to eliminate such striping entirely by reconstructing an appropriate subset of radial data that excludes the minority of degraded views.

We initially assumed that a golden view angle increment would prove optimal for radial UnQISS. However, the large inter-view jumps in gradient amplitude produced eddy current-related image artifacts for the outer slices in each table station. These jumps are avoided using a smaller optimized view angle increment. With a view angle increment ≈10 degrees (versus ≈111.25 degrees for golden angle), the eddy current-related artifacts were eliminated.

Unlike ECG-gated QISS, UnQISS requires the use of inversion rather than saturation pulses to suppress background tissue and venous signal. Even with inversion pulses, venous signal tended to be more prominent with UnQISS. In order to further reduce venous signal, one could apply several thinner FOCI inversion pulses, which would improve the inversion slab profile, rather than a single broad inversion pulse. In addition, the venous inversion pulses do not need to be applied at the same time as the in-plane inversion pulses. Better venous suppression might be obtained by shifting the venous inversion pulses closer to the bSSFP readout.

Compared with QISS MRA and phased array coils for signal reception, the arterial SNR was lower using UnQISS MRA and the body coil for signal reception. Nonetheless, UnQISS image quality was adequate for demonstrating the entire length of the peripheral artery tree, including small caliber calf vessels. Still better image quality and spatial resolution are obtained using phased array coils. If a peripheral array coil is not available, standard phased array coils (e.g. body array or spine coil) can be used to optimize image quality for the calf,

ankle and foot vessels. A phased array coil is probably not needed for the larger vessels proximal to the popliteal trifurcation.

Because of the extended radial readout, UnQISS is not amenable to the use of fat saturation RF pulses. The current implementation of phase-based fat suppression requires off-line image processing, but could be implemented as an automated in-line process. Unlike chemical-shift and Dixon-based techniques, phase-based fat suppression does not eliminate partial volume averaging at fat/water interfaces. Such partial volume averaging might reduce the apparent caliber of small vessels in the calf region. Better image quality might be obtained by using other approaches for fat suppression that do not suffer from such partial volume averaging, such as alternating TR or Dixon-based techniques.[18,19] It might also prove feasible to use a spoiled gradient-echo readout instead of bSSFP, which would allow the use of conventional fat suppression techniques.

Finally, we opted to use long, fixed values for shot TR/QI/readout duration on the order of 2400 ms/1200 ms/1200 ms. Scan time can be reduced by using shorter values matched to the individual subject's RR interval. However, reducing the readout duration will also reduce SNR, which might marginalize image quality if the body coil is used for signal reception. For very slow heart rates with RR > 1200 ms, it might be necessary to lengthen the shot TR in order to avoid flow artifacts. However, further study will be required to determine if a longer shot TR is needed in this situation.

In conclusion, we have demonstrated that peripheral NEMRA can be obtained without the need for cardiac gating. Among the main benefits for UnQISS is the simple patient setup (no ECG leads; phased array coils are optional) and scanning procedure (no scout scan; scan parameters are not tailored for the individual patient). The method may be particularly helpful for patients with an irregular cardiac rhythm or large body habitus. Current drawbacks include increased scan time compared to the ECG-gated QISS technique, slightly increased venous signal, and the need for off-line image processing for phase-based fat suppression. With further technical optimization, it is anticipated that image quality and scan time will be further improved.

Acknowledgments

Work was supported in part by NIHR01HL096916 and a grant from The Grainger Foundation. We would like to thank Dr. Matthias Gunther for providing the code used to generate the FOCI RF pulses.

References

1. Kuo PH, Kanal E, Abu-Alfa AK, Cowper SE. Gadolinium-based MR contrast agents and nephrogenic systemic fibrosis. Radiology. 2007; 242:647–649. [PubMed: 17213364]
2. Brittain JH, Olcott EW, Szuba A, Gold GE, Wright GA, Irarrazaval P, Nishimura DG. Three-dimensional flow-independent peripheral angiography. Magn Reson Med. 1997; 38:343–354. [PubMed: 9339435]
3. Katoh M, Buecker A, Stuber M, Günther RW, Spuentrup E. Free-breathing renal MR angiography with steady-state free-precession (SSFP) and slab-selective spin inversion: initial results. Kidney Int. 2004; 66:1272–1278. [PubMed: 15327427]

4. Priest AN, Graves MJ, Lomas DJ. Non-contrast-enhanced vascular magnetic resonance imaging using flow-dependent preparation with subtraction. Magn Reson Med. 2012; 67:628–637. [PubMed: 21713977]
5. Miyazaki M, Lee VS. Nonenhanced MR angiography. Radiology. 2008; 248:20–43. [PubMed: 18566168]
6. Miyazaki M, Takai H, Sugiura S, Wada H, Kuwahara R, Urata J. Peripheral MR angiography: separation of arteries from veins with flow-spoiled gradient pulses in electrocardiography-triggered three-dimensional half-Fourier fast spin-echo imaging. Radiology. 2003; 227:890–896. [PubMed: 12702824]
7. Fan Z, Sheehan J, Bi X, Liu X, Carr J, Li D. 3D noncontrast MR angiography of the distal lower extremities using flow-sensitive dephasing (FSD)-prepared balanced SSFP. Magn Reson Med. 2009; 62:1523–1532. [PubMed: 19877278]
8. Hodnett PA, Koktzoglou I, Davarpanah AH, et al. Evaluation of peripheral arterial disease with nonenhanced quiescent-interval single shot MR angiography. Radiology. 2011; 260:282–293. [PubMed: 21502384]
9. Edelman RR, Sheehan JJ, Dunkle E, Schindler N, Carr J, Koktzoglou I. Quiescent-interval single-shot unenhanced magnetic resonance angiography of peripheral vascular disease: technical considerations and clinical feasibility. Magn Reson Med. 2010; 63:951–958. [PubMed: 20373396]
10. Vosshenrich R, Kopka L, Castillo E, Böttcher U, Graessner J, Grabbe E. Electrocardiograph-triggered two-dimensional time-of-flight versus optimized contrast-enhanced three-dimensional MR angiography of the peripheral arteries. Magn Reson Imaging. 1998; 16:887–892. [PubMed: 9814770]
11. Markl M, Pelc NJ. On flow effects in balanced steady-state free precession imaging: pictorial description, parameter dependence, and clinical implications. J Magn Reson Imaging. 2004; 20:697–705. [PubMed: 15390233]
12. Ordidge RJ, Wylezinska M, Hugg JW, Butterworth E, Franconi F. Frequency offset corrected inversion (FOCI) pulses for use in localized spectroscopy. Magn Reson Med. 1996; 36:562–566. [PubMed: 8892208]
13. Payne GS, Leach MO. Implementation and evaluation of frequency offset corrected inversion [FOCI) pulses on a clinical MR system. Magn Reson Med. 1997; 38:828–833. [PubMed: 9358458]
14. Edelman RR, Giri S, Dunkle E, Galizia M, Amin P, Koktzoglou I. Quiescent-inflow single-shot magnetic resonance angiography using a highly undersampled radial k-space trajectory. Magn Reson Med. 2013; 70:1662–1668. [PubMed: 23348595]
15. Hargreaves BA, Vasanawala SS, Nayak KS, Hu BS, Nishimura DG. Fat-suppressed steady-state free precession imaging using phase detection. Magn Reson Med. 2003; 50:210–213. [PubMed: 12815698]
16. Baum RA, Rutter CM, Sunshine JH, Blebea JS, Blebea J, Carpenter JP, Dickey KW, Quinn SF, Gomes AS, Grist TM, et al. Multicenter trial to evaluate vascular magnetic resonance angiography of the lower extremity. American College of Radiology Rapid Technology Assessment Group. JAMA. 1995; 274:875–880. [PubMed: 7674500]
17. Meaney JF, Ridgway JP, Chakraverty S, Robertson I, Kessel D, Radjenovic A, Kouwenhoven M, Kassner A, Smith MA. Stepping-table gadolinium-enhanced digital subtraction MR angiography of the aorta and lower extremity arteries: preliminary experience. Radiology. 1999; 211:59–67. [PubMed: 10189454]
18. Leupold J, Hennig J, Scheffler K. Alternating repetition time balanced steady state free precession. Magn Reson Med. 2006; 55:557–565. [PubMed: 16447171]
19. Huang TY, Chung HW, Wang FN, Ko CW, Chen CY. Fat and water separation in balanced steady state free precession using the Dixon method. Magn Reson Med. 2004; 51:243–247. [PubMed: 14755647]

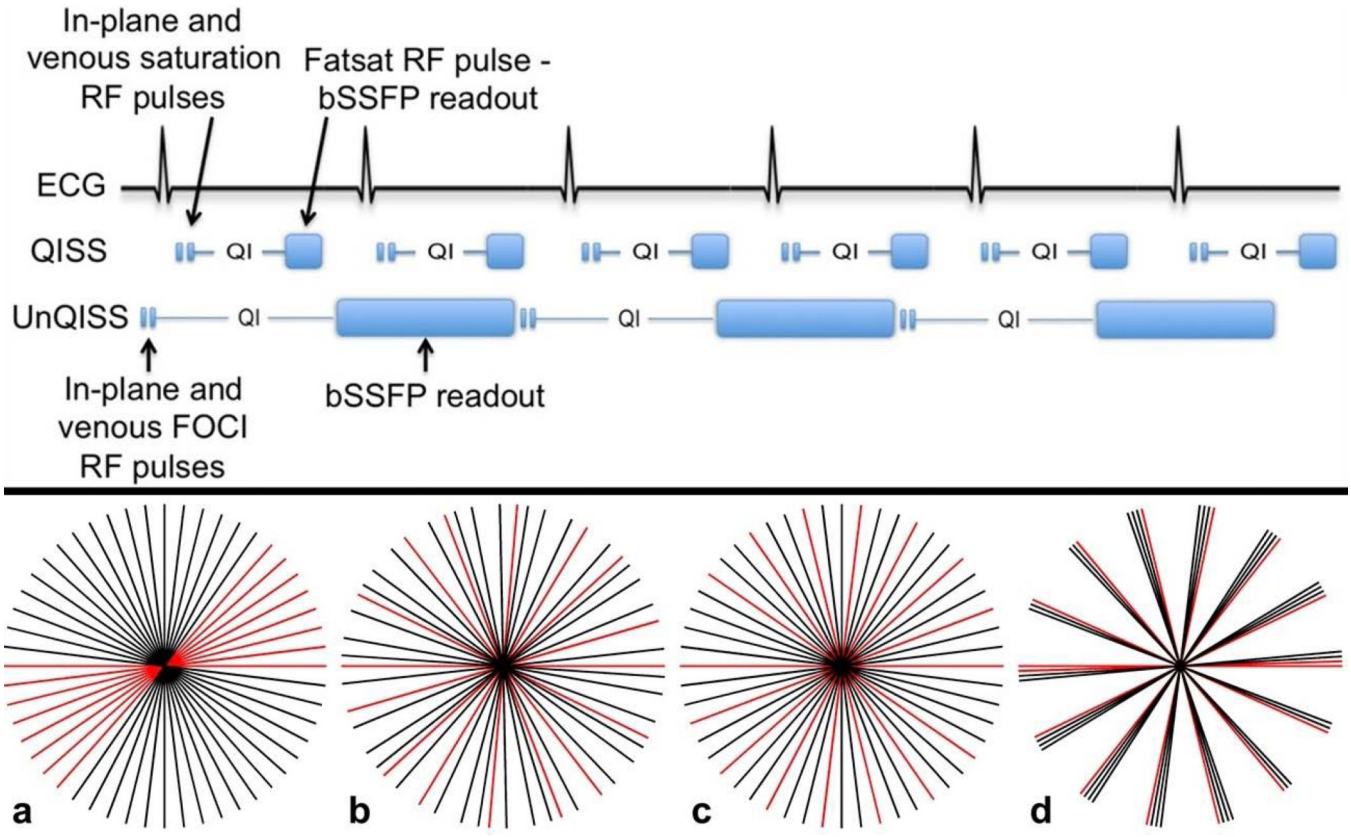

Figure 1.

Top: Illustration of the differences between ECG-gated QISS MRA and UnQISS MRA. Compared with ECG-gated QISS MRA, UnQISS MRA is not synchronized to the cardiac cycle, uses FOCI inversion pulses instead of saturation pulses to suppress in-plane tissue and venous signals, uses much lengthier QI and bSSFP readout, and phase-based fat suppression instead of a chemical shift-selective fat saturation pulse.

Bottom: Azimuthal coverage for an UnQISS scan acquiring 26 views per shot with eight views (red) that are degraded by flow artifacts. (a) Linear azimuthal angle increment (6.92308 degrees), (b) golden angle increment (111.24612 degrees), (c) optimized azimuthal equidistant projections making multiple revolutions around radial k-space (increment of 20.76923 degrees, $m = 3$), and (d) non-optimized view angle increment (25.96154 degrees). The most uniform k-space coverage is provided by optimized azimuthal equidistant projections. The views containing artifactual signal fluctuations are well distributed using both the golden and optimized azimuthal angle increments, but are bunched together with the linear increment.

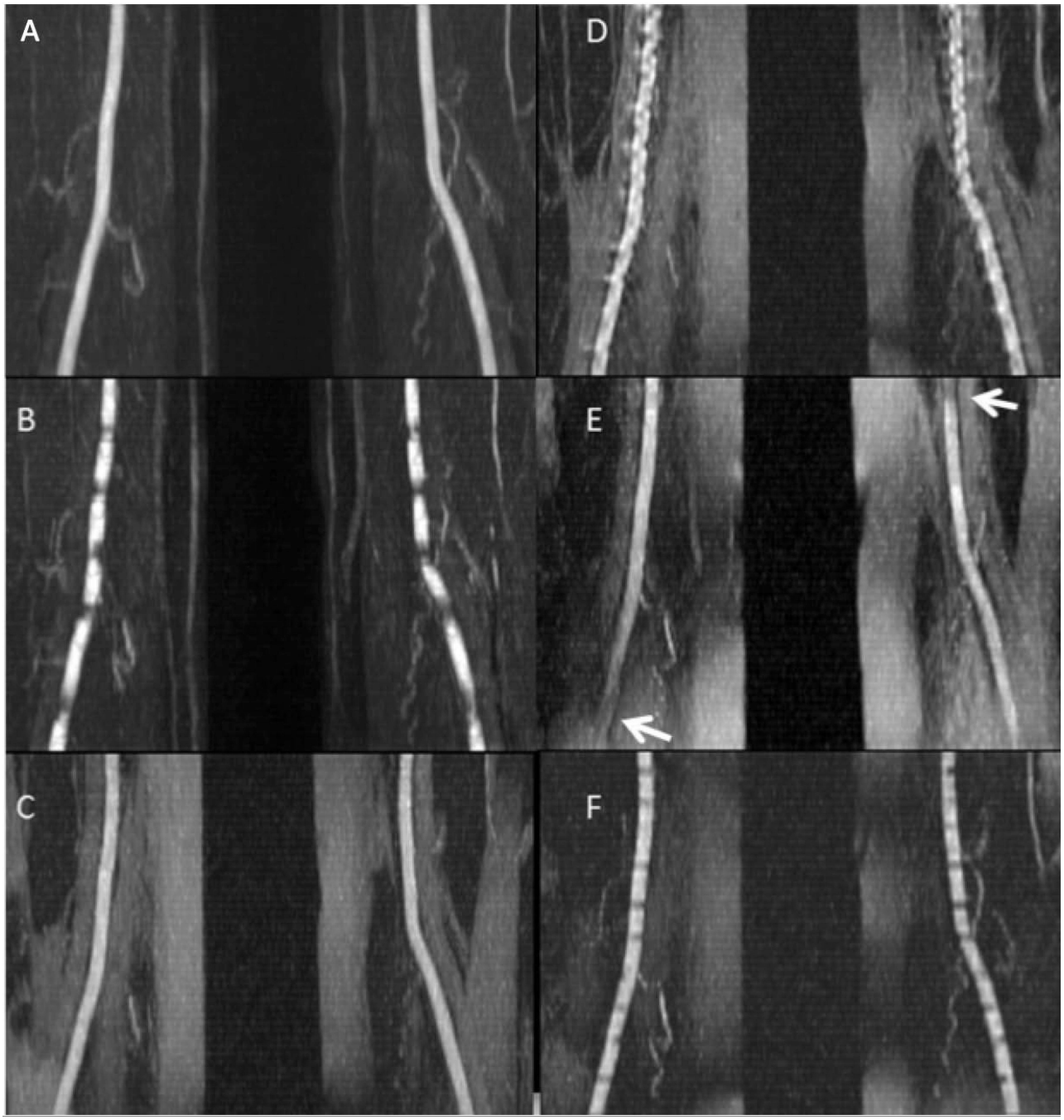

Figure 2.

40 mm-thick maximum intensity projections for QISS and UnQISS acquired in a healthy subject with RR ~760 ms. QISS was acquired with the peripheral vascular coil and fat saturation, sampling bandwidth = 646 Hz/pixel and 92 views. UnQISS was acquired using the body coil without fat suppression, sampling bandwidth 651 Hz/pixel and 316 views. **(a)** ECG-gated QISS shows uniform arterial signal. **(b)** QISS (QI = 228 ms) acquired without ECG gating shows horizontal banding artifacts. **(c)** UnQISS acquired with shot TR/QI = 2400 ms/1200 ms, radial k-space trajectory and a view angle increment (9.68353 degrees, *m*

= 17) shows the arteries comparably to ECG-gated QISS (although with higher fat signal since phase-based fat suppression was not used). **(d)** UnQISS acquired with identical imaging parameters to (c) except for using a Cartesian k-space trajectory shows severe, artifactual vessel irregularities. **(e)** UnQISS acquired with identical imaging parameters to (c) except for using a golden view angle increment (111.24612 degrees) shows loss of arterial signal (arrows) in the lower left and upper right corners of the image. **(f)** UnQISS acquired using shorter shot TR/QI values of 1716 ms/25 ms (TI = 625 ms) shows horizontal banding artifacts.

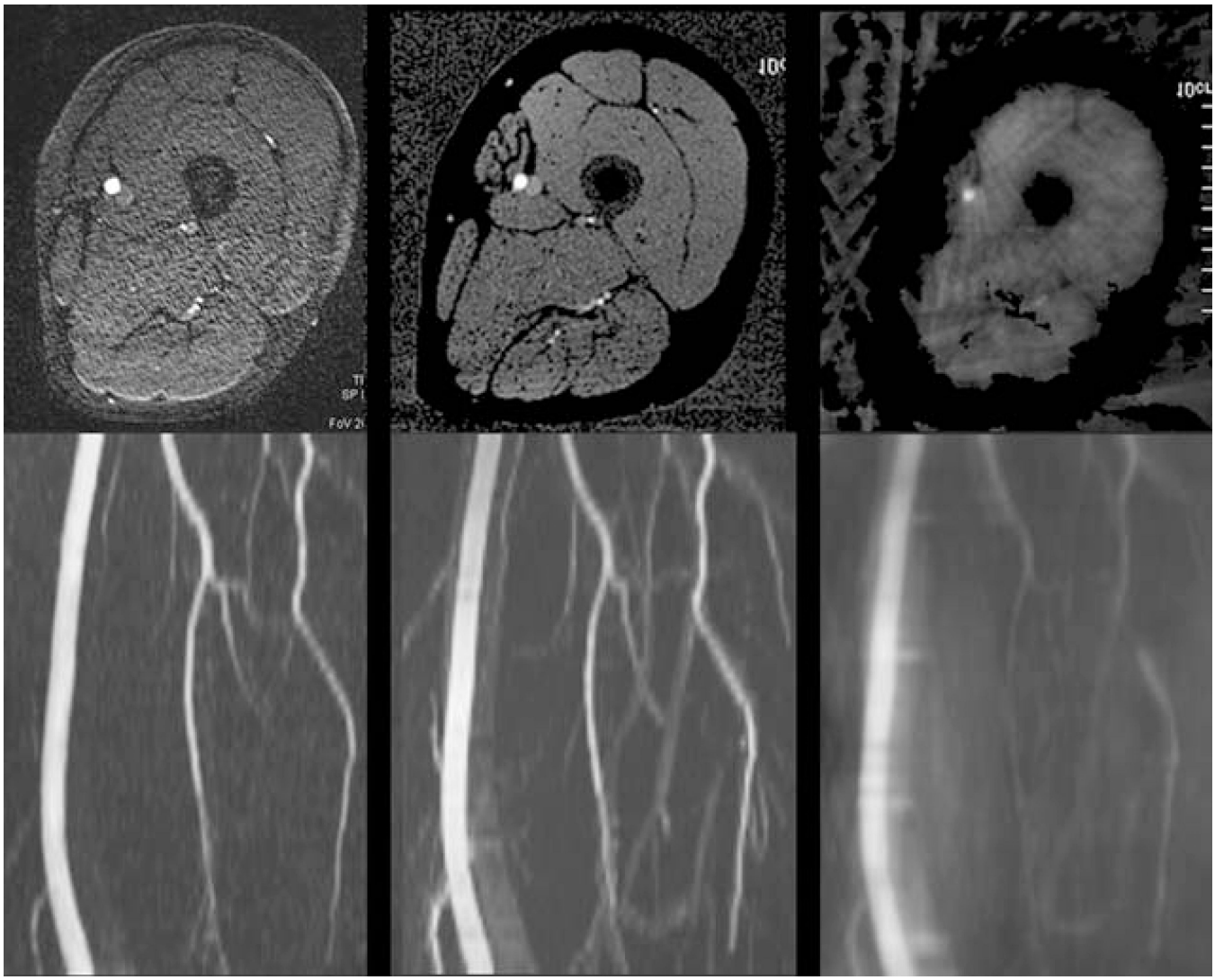

Figure 3.

Impact of azimuthal view angle increment. Top row: Axial images; bottom row: corresponding MIP images. (Left) ECG-gated Cartesian QISS image with 92 views; (middle) UnQISS image with 316 views using an optimal azimuthal view angle increment (9.68353 degrees, $m = 7$); (right) UnQISS image using a non-optimal view angle increment (9.47368 degrees) shows severe artifacts from non-uniform radial k-space sampling. All images were obtained using phased array coils; UnQISS used phase-based fat suppression.

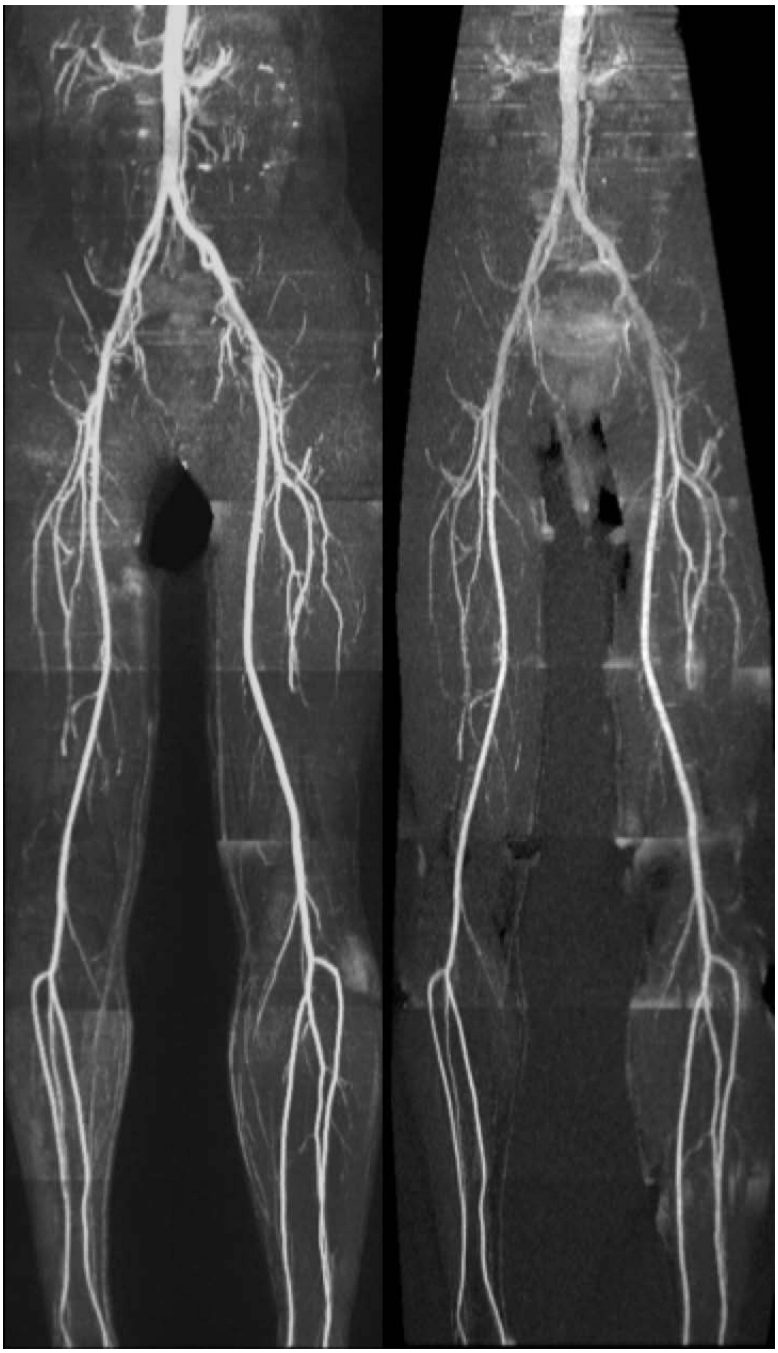

Figure 4.

Peripheral MRA in a healthy subject. Comparison of whole-leg ECG-gated QISS (left) with UnQISS MRA (right) using 3 mm slice thickness and 1 mm in-plane spatial resolution. QISS was acquired with peripheral vascular coil, body and spine phased array coils, using a Cartesian k-space trajectory with repetition time equal to the RR interval. UnQISS was acquired using the body coil only, shot TR = 2.4 sec, radial acquisition with optimized azimuthal equidistant projections, sampling bandwidth 651 Hz/pixel, 316 views.

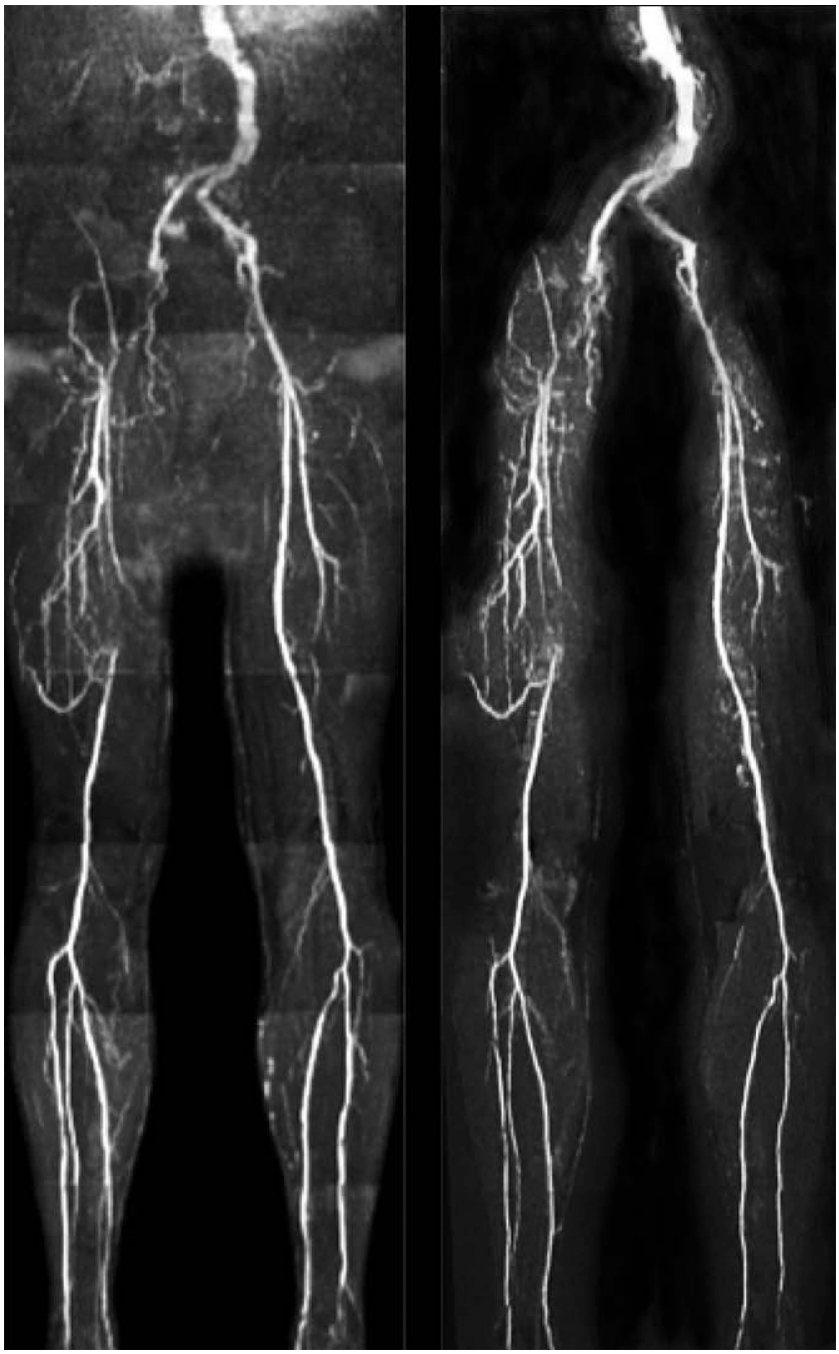

Figure 5.
Patient with multi-focal PAD. Occlusions of the right external iliac and superficial femoral arteries and associated collaterals are comparably demonstrated by UnQISS (right) and QISS (left), as is the occlusion of the left anterior tibial artery.

Table 1

Summary of imaging parameters for QISS and UnQISS.

Parameter	QISS	UnQISS
Sampling bandwidth	658 Hz/pixel	651 Hz/pixel
Cardiac gating	ECG	None
Shot TR	RR interval	2400 ms
Intra-view TR	3.8 ms	3.5 ms
TI/QI	350 ms/228 ms	1800 ms/1200 ms
Spatial resolution	3 mm × 1mm × 1mm	3 mm × 1mm × 1mm
K-space trajectory	Cartesian	Radial using optimized azimuthal view angles
Acceleration	GRAPPA 2, 5/8 partial Fourier	None
Venous suppression	Sinc RF pulse, 100 mm thickness	FOCI RF pulse, 200 mm thickness
In-plane suppression	Sinc RF pulse, 6 mm thickness	FOCI RF pulse, 6 mm thickness
Fat suppression	Chemical shift selective RF pulse	Phase-based
RF coils	Phased array coils	Body coil or phased array coils
Scan time/station	48 sec for RR of 1 sec (depends on heart rate)	115 sec (independent of heart rate)